Reducing eccentricity in black-hole binary evolutions with initial parameters from post-Newtonian inspiral

Sascha Husa, Mark Hannam, José A. González, Ulrich Sperhake, Bernd Brügmann Theoretical Physics Institute, University of Jena, 07743 Jena, Germany

Standard choices of quasi-circular orbit parameters for black-hole binary evolutions result in eccentric inspiral. We introduce a conceptually simple method, which is to integrate the post-Newtonian equations of motion through hundreds of orbits, and read off the values of the momenta at the separation at which we wish to start a fully general relativistic numerical evolution. For the particular case of non-spinning equal-mass inspiral with an initial coordinate separation of D=11M we show that this approach reduces the eccentricity by at least a factor of five to e<0.002 as compared to using standard quasi-circular initial parameters.

PACS numbers: 04.25.Dm, 04.30.Db, 95.30.Sf, 98.80.Jk

I. INTRODUCTION

Recent breakthroughs in numerical relativity [1, 2, 3] have made it possible to accurately simulate the last orbits, merger and ringdown of a black-hole binary system, and to compute the gravitational waves emitted in the process. Comparison of these waveforms with those produced by analytic techniques (i.e., post-Newtonian [PN] methods) has already begun [4, 5, 6, 7, 8, 9], as has the process of preparing these waveforms for use in gravitational-wave searches [8, 9]. We would like to start the comparison and template-building process with binaries that undergo non-eccentric inspiral, but many of these simulations model systems with non-zero eccentricity. This is ironically due to the use of "quasicircular orbit" initial momenta, which are based on an approximate circularity condition. However, a spiraling motion must contain a radial component. We wish to find initial tangential and radial momenta that, for a given initial separation, lead to non-eccentric inspiral.

Pfeiffer, et al. [10] recently suggested an iterative procedure to reduce eccentricity. They simulate a system with quasi-circular (QC) parameters for two orbits, measure the eccentricity, make an appropriate modification to the initial parameters (including the introduction of a radial component to the motion), and start the simulation again. They repeat this procedure until the eccentricity is reduced by a factor of ten. The drawback of their method is that it requires at least one "false start", which is computationally expensive, and, as pointed out in [10], it is not clear how to generalize the method to evolutions of spinning black holes, for which the blackhole separation and wave frequency will not in general be a monotonic function of time. We would rather find a general method to calculate low-eccentricity parameters from the outset.

In earlier papers we used a PN approximation to calculate QC parameters for equal-mass [11], unequal-mass [12] and spinning [13] black holes, and found that they compared well with parameters calculated using more sophisticated numerical methods [11]. In this paper we follow up on Miller's work [14] and use PN methods to

estimate initial parameters for low-eccentricity inspiral.

Our procedure is to numerically integrate the PN equations of motion (at the highest PN order available; see for example [15]) for two point particles over hundreds of orbits, and read off the particles' momenta when they have reached the separation we wish to use as an initial separation in a fully general relativistic numerical simulation. We use Mathematica for the integration, which typically takes several seconds. Note that we could instead use lower-order PN estimates of the radial momentum (for example by using the quadrupole formula), but we wish to obtain the most accurate results possible, and to use a method that can later be applied with some confidence to spinning binaries. A PN approach was also used to introduce a radial component to the motion in [16], although the details of the method were not given.

The key to this approach is to exploit the fact that any initial eccentricity will decay over time due to the circularizing effect of gravitational-wave emission, but on a time-scale of hundreds of orbits, not the < 10 orbits typically simulated by a numerical code. We therefore start the PN evolution at sufficiently large initial separation D (in practice D=40M) to allow radiation-reaction to circularize the orbits. (We will quote time and length in units of the total initial black-hole mass M; see [11].)

Given the parameters from PN inspiral, full GR numerical evolutions are then performed with the BAM code [11, 17], using the moving-puncture method [2, 3] to evolve Bowen-York initial data [18] in puncture form [19] and generated by a pseudo-spectral method [20]. In order to perform long evolutions with sufficient accuracy for the present purpose, it was crucial to modify our previous evolution algorithm to use sixth order accurate derivative operators [21], instead of the more standard fourth-order accurate choice.

We find that the PN-inspired initial momenta lead to evolutions with at least five times less eccentricity than their QC counterparts.

In Section II we summarize the PN equations that we use and the method to integrate them. In Section III we present results from simulations of an equal-mass binary.

II. INTEGRATION OF THE PN EQUATIONS OF MOTION

We have used the PN equations of motion as described in [15] in the ADMTT gauge. We have implemented both the usual Taylor-expanded and the effective-one-body (EOB) versions of the Hamiltonian; the calculations presented here are however all based on the Taylor-expanded version. The PN solution in the ADMTT gauge for a two-body system agrees with our Bowen-York puncture initial data up to 2PN order (see, for example, the explicit solutions in Appendix A of [22]). The conservative part of the Hamiltonian is given up to third PN order, and was originally derived in [22, 23, 24], see also [25, 26, 27]. Radiation-reaction flux terms are calculated up to 3.5PN order beyond the quadrupole order, which is achieved by averaging the radiation flux over one orbit, assuming quasi-circular inspiral [28, 29, 30]. We have also included the leading-order spin-spin and spin-orbit coupling terms for the conservative part of the Hamiltonian [31, 32, 33], and spin-induced radiation flux terms as described in [15] (and again averaged over one orbit).

In the nonspinning case the PN equations of motion are a system of six coupled ordinary differential equations of the form

$$\frac{dx^i}{dt} = \frac{\partial H}{\partial p_i},\tag{1}$$

$$\frac{dp_i}{dt} = -\frac{\partial H}{\partial x^i} + F_i, \tag{2}$$

where H is the PN-Hamiltonian (responsible for the conservative part of the dynamics), x^i is the separation vector between the two particles and p^i is the momentum of one particle in the center-of-mass frame. In the spinning case the system is augmented by the evolution equations for the spins. The quantity F_i is the radiation-reaction flux term. We have used the evolution equations precisely in the form presented in [15].

Starting at a suitably large initial separation (D=40M is used in practice for an equal-mass binary), initial momenta are chosen using the 3PN formula given in [11]. We have checked that D=20M would be somewhat too close — small oscillations in the radius are still visible at D=11M, where we wish to start the evolution of the full Einstein equations; see Fig. (1). Integrating the PN equations from D=100M (2071.5 orbits) makes very little difference for the inspiral parameters. For the full numerical evolution to start at D=11M the tangential component of the momentum would change by $4\times10^{-4}\%$, the radial component by 0.2% as compared to using a PN-inspiral from D=40M.

The equations are then integrated in Mathematica 5.2 using the NDSolve function with different options for the integration algorithm, tolerance levels and internal precision to check the accuracy of the results. Mathematica stops the integration automatically when the PN equations of motion become ill-defined. Several consistency checks are applied to make sure the correct equations are

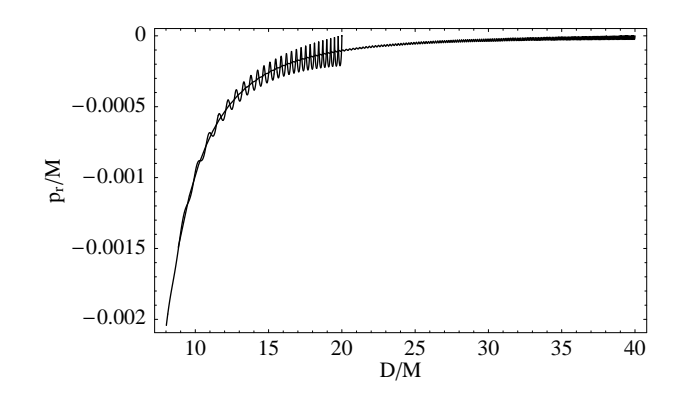


FIG. 1: The radial momentum component is plotted versus separation for PN-inspirals starting from D=20M and D=40M. A separation of D=20M is clearly not sufficient to produce non-eccentric inspiral parameters, since small oscillations can still be seen at D=11M, while for D=40M the initial eccentricity has essentially decayed away.

integrated: When radiation reaction is switched off, energy and angular momentum should be constant up to numerical error. To check this, we integrate the conservative equations of motion with initial separations 40M and 50M for about 200 orbits and monitor the relative decay of energy and angular momentum, which remain below 3.5×10^{-6} for the NDSolve options we have used for the results presented here. When radiation reaction is switched on, the PN equations of motion imply the identity

$$\frac{dE}{dt} = \frac{d\varphi}{dt} \boldsymbol{\lambda} \cdot \left\langle \frac{d\boldsymbol{J}}{dt} \right\rangle,$$

in the circular equal-mass case [15], where φ is the orbital phase, λ the time independent unit vector in the direction of the orbital angular momentum, and $\langle \cdot \rangle$ denotes the orbital average. We have checked that for the actual inspiral (which is not exactly circular) this equation (without taking the orbital average) is satisfied to better than 2×10^{-4} over the entire inspiral.

The system displays some initial eccentricity, but this decays and by the time the particles are at a separation suitable for a numerical evolution (i.e., D < 20M), the inspiral has negligible eccentricity, as shown in Fig. (1). Similar plots are also shown in [14].

We now wish to perform a full GR numerical evolution of the last orbits of the binary system. The puncture initial data solver requires as input the black hole's masses, positions, and momenta. Given the masses and some desired initial separation, we can read off the appropriate momenta from the integrated solution $(x^i(t), p^i(t))$ of the PN equations of motion.

Configuration	P_x/M	P_y/M	e_D	e_{ω}
QC11	∓ 0.0899395	0	0.012	0.01
E11	∓ 0.0900993	$\mp 7.09412 \times 10^{-4}$	0.002	0.002

TABLE I: Initial physical parameters for a standard "quasicircular orbit" (QC11) and PN-inspired low-eccentricity (E11) configuration. Both have an initial coordinate separation of D=11M and the punctures are placed at $y=\pm 5.5M$. The initial eccentricities e_D and e_ω are estimated using Eqns. (3) and (4).

III. NUMERICAL RESULTS

We consider the configurations shown in Table I. The black-hole punctures are placed at an initial separation of D=11M. They are given either quasi-circular orbit (QC) parameters as estimated from the 2PN-accurate expression in [34, 35], or the PN-inspired low-eccentricity parameters described in Section II. When evolved both initial configurations lead to about seven orbits before merger.

In the notation of [11], the data were evolved with a grid setup of $\chi_{\eta=2}[5\times64:5\times128:6]$ using the sixth-order accurate spatial finite differencing stencils, as described in detail in [21]. Lower-resolution runs and convergence tests show that the simulations are cleanly sixth-order convergent up to around 1000M of evolution time and drop slightly in convergence order after that. In this paper we only need the simulation up to t=1000M, at which time the uncertainty in D(t) is 0.6%; for all earlier times it is lower.

Figure 2 shows the coordinate separation of the punctures as a function of time, for simulations with the QC11 and E11 initial parameters. The figure begins at t=257M, the time at which the binary completes one orbit. Before that time there are oscillations in D(t) due to gauge adjustments; the initially stationary punctures pick up speed, the lapse and shift adapt to the dynamical gauge conditions, and the numerical grid points rapidly retract from the extra asymptotically flat ends in the puncture initial data [36, 37]. All of these effects preclude a meaningful estimate of the eccentricity during the first orbit. The figure ends at t=1050M, when the system has completed a further four orbits. We can clearly see oscillations due to eccentricity in the QC11 data, while the E11 data appears relatively eccentricity-free.

We use two methods to estimate the eccentricity, as also used in [4, 5, 10]. Assume that we know the zero-eccentricity quasi-circular inspiral for our system, and denote the corresponding coordinate separation of the punctures as a function of time as $D_c(t)$ and the orbital frequency as $\omega_c(t)$. The coordinate separation and orbital frequency for any given numerical evolution are D(t) and $\omega(t)$. The eccentricity can be estimated by extrema in

either

$$e_D(t) = \frac{D(t) - D_c(t)}{D_c(t)},$$
 (3)

or

$$e_{\omega}(t) = \frac{\omega(t) - \omega_c(t)}{2\omega_c(t)}.$$
 (4)

In practice we estimate $D_c(t)$ by fitting a curve through the numerical D(t) for the low-eccentricity simulation

$$D_c(t) = aT^{1/2} + bT + cT^{3/2} + dT^2, (5)$$

where $T = T_M - t$ and T_M is a rough estimate of the merger time. For the E11 simulation, we choose $t_M = 1270M$. Similarly we follow [5] and fit a fourth-order polynomial in time through the $\omega(t)$ curve for the low-eccentricity simulation and obtain $\omega_c(t)$.

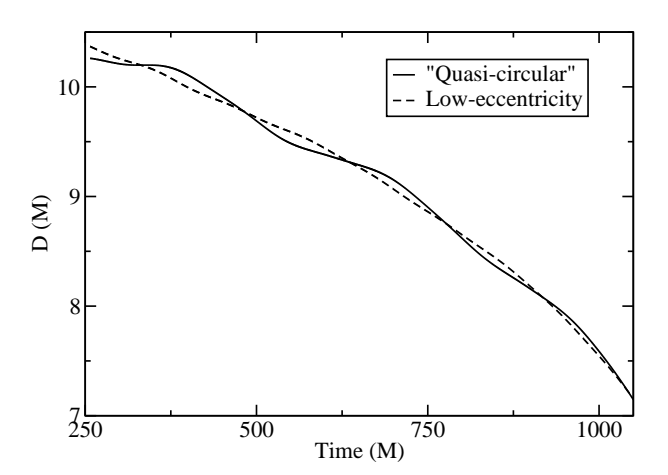
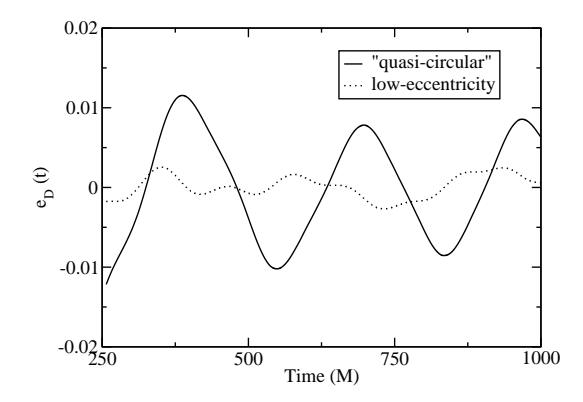


FIG. 2: Coordinate separation of the punctures as a function of time for the quasi-circular (QC11) and PN-inspired low-eccentricity (E11) initial parameters.

For the quasi-circular simulation QC11, Eqn. (3) gives $e_D = 0.012 \pm 0.002$ and Eqn. (4) gives $e_\omega = 0.01 \pm 0.001$. The uncertainties are estimated by repeating the calculation with curves $D_c(t)$ and $\omega_c(t)$ fit through the eccentric QC11 data. Note that the frequency method (4) gives a lower value than the separation method (3); similar results were found in [4, 10].

For the low-eccentricity E11 simulation, we find $e_D=0.002\pm0.001$ and $e_\omega=0.002\pm0.0005$. The large uncertainty in the value from the separation method is due to the larger uncertainty in the curve fit through D(t). For both estimates, however, the one firm conclusion we can draw is that the eccentricity in the E11 simulation is significantly lower (by a factor of at least five or six) than that for the QC11 simulation.

The functions $e_D(t)$ and $e_\omega(t)$ are shown in Figure 3. For the QC11 simulations we see clear oscillations due to the eccentricity. The curves for the E11 run are much noisier. This may be due to errors in the curve fit through the E11 D(t) and $\omega(t)$ being of a similar magnitude to the oscillations due to the remaining eccentricity.



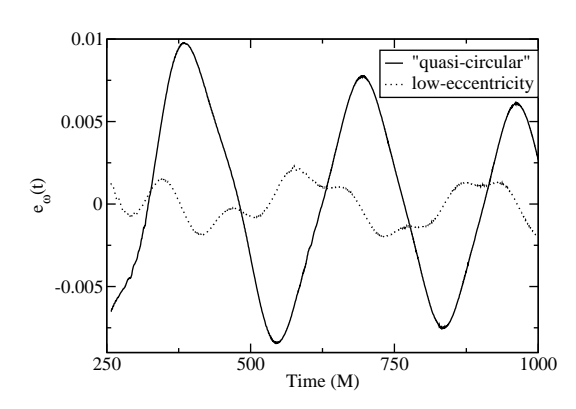


FIG. 3: The functions $e_D(t)$ and $e_\omega(t)$ for the QC11 and E11 simulations. The extrema of these functions give an estimate of the eccentricity, as described in the text.

For convenience, we have computed analytical fits for the momentum parameters from our numerical solution to the PN evolution equations. These fits have been computed from a PN-inspiral starting at D=100M. With the expressions

$$\dot{r} = -2.7069 \left(1.21329 - \frac{1.5053}{\sqrt{r}} + \frac{2.60155}{r} \right) r^{-2.993}$$

$$p_r = -1.9188 \left(1.76084 - \frac{5.3029}{\sqrt{r}} + \frac{9.06417}{r} \right) r^{-3.288}$$

$$p_t = \pm \left(P_{3PN}(r) - \frac{35.0988}{r^{5.36702}} \right)$$

the relative errors with respect to our numerical results are smaller than 0.3% for \dot{r} and p_r and 3.5×10^{-4} for p_t over the range D=8M to D=20M. Here $P_{3PN}(r)$ is the 3PN-accurate quasi-circular value, which we have

separation/M	$-\dot{r} \ (\times 10^{-3})$	$-p_r/M \ (\times 10^{-3})$	p_t/M
8.0	5.3857	2.0906	0.112349
8.5	4.4944	1.7023	0.107614
9.0	3.7839	1.4019	0.103376
9.5	3.2133	1.1670	0.099561
10.0	2.7512	0.9813	0.096109
10.5	2.3736	0.8328	0.092968
11.0	2.0624	0.7128	0.090099
11.5	1.8039	0.6150	0.087464
12.0	1.5872	0.5343	0.085037
12.5	1.4042	0.4672	0.082791
13.0	1.2487	0.4110	0.080706
13.5	1.1156	0.3635	0.078765
14.0	1.0010	0.3231	0.076952
14.5	0.9018	0.2886	0.075255
15.0	0.8155	0.2589	0.073661
15.5	0.7398	0.2331	0.072161
16.0	0.6734	0.2106	0.070746
16.5	0.6150	0.1911	0.069409
17.0	0.5629	0.1738	0.068143
17.5	0.5169	0.1586	0.066942
18.0	0.4757	0.1452	0.065801
18.5	0.4386	0.1331	0.064715
19.0	0.4055	0.1224	0.063679
19.5	0.3757	0.1129	0.062691
20.0	0.3488	0.1043	0.061747

TABLE II: Radial velocity and radial (p_r) and tangential (p_t) components of the black hole momentum as a function of the separation in ADMTT coordinates for selected values of the separation. The numbers have been produced from a PN-inspiral from D=100M.

used previously in [11]. In Table (II) we tabulate results for selected values of the black-hole separation.

IV. CONCLUSIONS

We have presented a conceptually simple method to specify very low eccentricity initial-data parameters for the numerical evolution of binary systems. We integrate PN equations of motion from an initial separation of D=40M to the separation we wish to use as the starting point for a numerical evolution of the full Einstein equations. Initial conditions for the PN inspiral are taken from a 3PN accurate circular orbit condition. These conditions lead to a small initial eccentricity that radiates away by the time we read off the parameters for our full GR numerical evolution.

The PN equations are accurate to 3PN order in the conservative part when neglecting spins. For spin-spin and spin-orbit interactions we have only implemented the leading order terms, although these were not used

in the application presented here. Radiation-reaction is implemented via averaging over orbits, and is accurate to 3.5PN order beyond the leading quadrupole contribution. The method can in principle be applied to general black-hole initial data, and applications to unequal-mass and spinning cases will be presented elsewhere.

We report in detail on an equal-mass inspiral, where the evolution of the full Einstein equations is started at a coordinate separation of D=11M [38]. Our method reduces the eccentricity by at least a factor of five to a value below e=0.002. Remaining oscillations in the coordinate distance of the two black holes cannot clearly be identified as eccentricity. We also provide a curve fit and table of low-eccentricity parameters for equal-mass binaries.

An important corollary from the success of this method is that the input parameters in the initial data construction ($\{m_i, p_i, D\}$ in the Bowen-York extrinsic curvature and conformal flatness ansatz) actually correspond to the physical properties of the black holes during a long-term evolution with excellent accuracy. One might instead have found that the presence of "junk" radiation spoils the initial data, and that after this radiation has left the system the dynamics of the black holes are very different from what one would have expected from, for example, a PN evolution with the same physical parameters. The fact that PN low-eccentricity parameters translate to

low-eccentricity numerical evolutions with Bowen-York puncture data suggest that neither the junk radiation nor the constraint-solution procedure adversely affect the physics of the system.

Pfeiffer, et al. [10] have shown that waveforms from quasi-circular and low-eccentricity parameters have large fitting factors (> 0.99 for $l \leq 4$ multipole contributions), and conclude that "quasi-circular" waveforms will be sufficiently useful for gravitational-wave detection. However, the use of waveforms with the lowest eccentricity possible will be necessary to make the most accurate matching possible to PN inspiral waveforms. Low-eccentricity waveforms were compared with PN waveforms in [5], and we will give a further detailed comparison in [39].

Acknowledgments

This work was supported in part by DFG grant SFB/Transregio 7 "Gravitational Wave Astronomy". We thank the DEISA Consortium (co-funded by the EU, FP6 project 508830), for support within the DEISA Extreme Computing Initiative (www.deisa.org). Computations were performed at LRZ (Munich) and at our inhouse Linux clusters Doppler and Kepler.

- [1] F. Pretorius, Phys. Rev. Lett. $\bf 95$, 121101 (2005), gr-qc/0507014.
- [2] M. Campanelli, C. O. Lousto, P. Marronetti, and Y. Zlochower, Phys. Rev. Lett. 96, 111101 (2006), gr-qc/0511048.
- [3] J. G. Baker, J. Centrella, D.-I. Choi, M. Koppitz, and J. van Meter, Phys. Rev. Lett. 96, 111102 (2006), gr-qc/0511103.
- [4] A. Buonanno, G. B. Cook, and F. Pretorius (2006), gr-qc/0610122, gr-qc/0610122.
- [5] J. G. Baker, J. R. van Meter, S. T. McWilliams, J. Centrella, and B. J. Kelly (2006), gr-qc/0612024.
- [6] M. Scheel (2007), presented at "NRm3PN Meeting", St. Louis.
- [7] E. Berti et al. (2007), gr-qc/0703053, gr-qc/0703053.
- [8] Y. Pan et al. (2007), arXiv:0704.1964 [gr-qc], arXiv:0704.1964 [gr-qc].
- [9] P. Ajith et al. (2007), arXiv:0704.3764 [gr-qc].
- [10] H. P. Pfeiffer, D. Brown, L. E. Kidder, L. Lindblom, G. Lovelance, and M. A. Scheel (2007), gr-qc/0702106.
- [11] B. Brügmann, J. A. González, M. Hannam, S. Husa, U. Sperhake, and W. Tichy (2006), gr-qc/0610128.
- [12] J. A. González, U. Sperhake, B. Brügmann, M. Hannam, and S. Husa, Phys. Rev. Lett. (2006), gr-qc/0610154.
- [13] J. A. Gonzalez, M. D. Hannam, U. Sperhake, B. Brügmann, and S. Husa (2007), gr-qc/0702052, gr-qc/0702052.
- [14] M. Miller, Phys. Rev. D $\mathbf{69}$, 124013 (2004), gr-qc/0305024.
- [15] A. Buonanno, Y. Chen, and T. Damour, Phys. Rev. D74,

- 104005 (2006), gr-qc/0508067.
- [16] M. Campanelli, C. O. Lousto, Y. Zlochower, and D. Merritt, Astrophys. J. 659, L5 (2007), gr-qc/0701164.
- [17] B. Brügmann, W. Tichy, and N. Jansen, Phys. Rev. Lett. 92, 211101 (2004), gr-qc/0312112.
- [18] J. M. Bowen and J. W. York, Phys. Rev. D 21, 2047 (1980).
- [19] S. Brandt and B. Brügmann, Phys. Rev. Lett. 78, 3606 (1997), gr-qc/9703066.
- [20] M. Ansorg, B. Brügmann, and W. Tichy, Phys. Rev. D 70, 064011 (2004), gr-qc/0404056.
- [21] S. Husa, J. A. González, M. Hannam, B. Brügmann, and U. Sperhake (2007), arXiv:0706.0740 [gr-qc].
- [22] P. Jaranowski and G. Schäfer, Phys. Rev. D 57, 7274 (1998).
- [23] T. Damour, P. Jaranowski, and G. Schäfer, Phys. Lett. B 513, 147 (2001), gr-qc/0105038.
- [24] T. Damour, P. Jaranowski, and G. Schafer, Phys. Rev. D62, 021501 (2000), erratum-ibid. 63, 029903, (2000), gr-qc/0003051.
- $[25]\,$ L. Blanchet and G. Faye, Phys. Rev. D $\mathbf{63},\,062005$ (2001).
- [26] V. C. de Andrade, L. Blanchet, and G. Faye, Class. Quant. Grav. 18, 753 (2001), gr-qc/0011063.
- [27] L. Blanchet and B. Iyer, Class. Quantum Grav. 20, 755 (2003), gr-qc/0209089.
- [28] L. Blanchet, Class. Quant. Grav. 15, 113 (1998), gr-qc/9710038.
- [29] L. Blanchet, B. R. Iyer, and B. Joguet, Phys. Rev. D 65, 064005 (2002), gr-qc/0105098.
- [30] L. Blanchet, T. Damour, G. Esposito-Farese, and B. R.

- Iyer, Phys. Rev. Lett. 93, 091101 (2004), gr-qc/0406012.
- [31] B. Barker and R. O'Connell, Phys. Rev. D 2, 1428 (1970).
- [32] B. Barker and R. O'Connell, Gen. Relativ. and Gravit. 5, 539 (1974).
- [33] B. Barker and R. O'Connell, Gen. Relativ. and Gravit. 11, 149 (1979).
- [34] L. E. Kidder, Phys. Rev. D ${\bf 52}$, 821 (1995), gr-qc/9506022.
- [35] B. Brügmann, J. A. González, M. Hannam, S. Husa, and U. Sperhake (2007), in preparation.
- [36] M. Hannam, S. Husa, D. Pollney, B. Brügmann, and

- N. Ó Murchadha (2006), gr-qc/0606099.
- [37] M. Hannam, S. Husa, N. Ó Murchadha, B. Brügmann, J. A. González, and U. Sperhake, Journal of Physics: Conference series (2007), in press, gr-qc/0612097.
- [38] R. Reiner, C. Guest, M. McKean, and H. Shearer, *This is spinal tap* (1984), "see also http://www.youtube.com/watch?v=akaD9v460y1", URL "http://www.imdb.com/title/tt0088258".
- [39] M. Hannam, S. Husa, J. A. González, U. Sperhake, and B. Brügmann (2007), in preparation.